Proceedings of the 17th World Congress
The International Federation of Automatic Control
Seoul, Korea, July 6-11, 2008

Self-scheduling controller for a launcher in atmospheric ascent

Saussié David [*,**] **Gianluigi Baldesi** [*,***] **Carsten Döll** [****]
Caroline Bérard [*,****]

[*] *SUPAERO, Toulouse, France*
[**] *Electrical engineering department, École Polytechnique de Montréal, Canada*
[***] *Dip. di Informatica e Sistemistica, Via Eudossiana18, 00184 Rome, Italy*
[****] *ONERA, DCSD, Toulouse, France*[⋆]

Abstract: This paper describes the synthesis of a self-scheduled controller for a launcher vehicle. The problem consists in designing a control law which will be valid on the atmospheric ascent trajectory, from time $5s$ to time $85s$ after takeoff, while ensuring decoupling performances for roll rates between $0°/s$ and $30°/s$. Eigenstructure assignment has been retained in its multi model approach. After introducing the problem itself and the launcher model, the theory related to self-scheduling synthesis is reviewed before its application on the launcher is described. A first performance analysis will be carried out to validate the method and the given results.

1. INTRODUCTION

As a standard practice, the control design for a launch vehicle is based on decoupled dynamic models. Several Thrust Vector Control (TVC) law designs, which assume that an action on the pitch plane produces no effect on the yaw plane, can be easily found in the literature (Alazard et al. [2003]). Coupling effects (Sadray and Colgreb [2005]) in the dynamics can be due to the external forces, but also to the state variables for the velocity linear components and the angular rate components. As Roux and Cruciani [2007] have presented, there can be cases where a no negligible roll rate can be foreseen. Therefore in order to keep valid the assumption of two uncoupled axes, a dedicated roll control system is added to the initial control design to reduce the roll rate. This additional subsystem has an important effect on the mass performance of the whole launch vehicle since it is added on the first stage.

In this paper the synthesis of a self-scheduled controller for a launcher vehicle having a no neglegible roll rate is presented. The coupled dynamics are decoupled for roll rates between $0°/s$ and $30°/s$ during the complete atmospheric flight using an eigenstructure assignment technique without the need of an additional roll control system. The (Mu-μ) iteration based on a worst-case analysis and multi-model eigenstructure assignment has given interesting results.

2. ROBUST MODAL CONTROL

2.1 Eigenstructure assignment

We briefly present here the classical eigenstructure assignment method that will be used in the first step to find the initial controller K_0 for the nominal plant. Let us consider a linear system (A_0, B_0, C_0, D_0) with n states, m inputs and p outputs.

⋆ E-mails: david.saussie@polymtl.ca, gianluigi.baldesi@gmail.com, carsten.doll@cert.fr, caroline.berard@supaero.fr

Proposition 1. Magni [2002] The triplet $T_i = (\lambda_i, v_i, w_i)$ satisfying

$$[\, A_0 - \lambda_i I \;\; B_0 \,] \begin{pmatrix} v_i \\ w_i \end{pmatrix} = 0 \tag{1}$$

is assigned by the static feedback K_0 if and only if

$$K_0 \,(\, C v_i + D w_i \,) = w_i \tag{2}$$

The input directions w_i and right eigenvectors v_i associated with the closed loop eigenvalue λ_i can be fixed by various methods. They can be chosen with decoupling objectives:

$$\begin{bmatrix} A_0 - \lambda_i I & B_0 \\ E & F \end{bmatrix} \begin{pmatrix} v_i \\ w_i \end{pmatrix} = 0 \tag{3}$$

with for example $E = e_j$ and $F = [0 \cdots 0]$ if the i^{th} mode must not excite the j^{th} state. More on the subject can be found in Magni et al. [1998].

2.2 Multi-model modal control

Multi-model eigenstructure assignment Magni et al. [1998] is done by simultaneously assigning triplets T_i for several models which reduces to solve a set of equality constraints of type (2). The choice of the models to treat with and the triplets to assign is determined by an analysis of the stability and/or performance robustness. The proposed iterative procedure is called (Mu-μ)-iteration for Multimodel-worst case analysis.

Procedure: (Mu-μ)-iteration

Step A.1 — Elaborate a first initial design on a nominal model. All kinds of synthesis methods can be applied at this step (H_∞ control, LQG optimal control , μ-synthesis, etc...). In the case of initial non-modal approaches, look for eigenstructure assignment having the same characteristics as the initial controller. Here, we will assign an eigenstructure which stems from a LQ design.

Step B.1 — Here, proceed with a classical multi-model analysis of the pole map and time-responses for worst case performance analysis. Real μ-analysis as proposed in Packard and Doyle [1993], Magni and Döll [1997] could be applied at this stage if an LFT was available. That is where the name (Mu-μ) stems from. If the initial design is satisfactory for all models or all values of uncertainties, then **stop**. Otherwise identify the worst-case model, determine its critical triplet T_i and continue with **Step B.2**.

Step B.2 — Improve the behaviour of the worst-case model by replacing the triplet T_i by T_i^* respecting the specifications while preserving the properties of all models treated before. You will need additional degrees of freedom which can be introduced by using dynamic controllers or self-scheduled controllers, see §2.3. Return to **Step B.1**.

Remark: See Magni [1999] for some general rules on multi-model eigenstructure assignment, for example to avoid incompatible assignments we should treat models as 'far' as possible from each other in the considered parameter space and/or relax some constraints on models treated before.

2.3 Multi-model modal self-scheduling

Classical gain-scheduling is typically done by interpolating *a posteriori* the linear controllers obtained for several models. But, because of structure, the gain-scheduling problem can be difficult to tackle. Multi-model modal control handles this task by choosing *a priori* the interpolation formula for the controller gain. This choice can be guided by physical constraints or previous experiments. Let us for example take a scheduling w.r.t measurable parameter δ and an interpolation formula

$$K_s(\delta) = K_0 + \delta K_1 + \delta^2 K_2 \tag{4}$$

The synthesis of this controller can then be tackled using the following Proposition 2 (Magni [2002]).

Proposition 2. The determination of such a self-scheduled controller is equivalent to the synthesis of a multi-model modal controller

$$K = [\, K_0 \;\; K_1 \;\; K_2 \,] \tag{5}$$

with respect to the augmented system

$$\left[A, B, \begin{pmatrix} C \\ \delta C \\ \delta^2 C \end{pmatrix}, \begin{pmatrix} D \\ \delta D \\ \delta^2 D \end{pmatrix} \right] \tag{6}$$

As it can be seen, the problem boils down to increasing the number of outputs of the original system (A, B, C, D) from p to $3p$. The augmentation of the ouput number offers the additional degrees of freedom necessary for the simultaneous resolution of some linear constraints of type (2) at **Step B.2** of the (Mu-μ)-iterations.

For aeronautical applications, refer Döll et al. [2001] and Constant et al. [2002].

3. APPLICATION TO THE LAUNCHER

Let us apply this method to the launcher atmospheric ascent problem.

3.1 Launcher model

Launch vehicle dynamics are generally described by 'short-period' equations of motion during the atmospheric flight. Indeed, in this particular flight phase, the main constraint for a launcher is to minimize the angle of attack, which generates a lift force acting on the lateral direction of vehicle. Therefore no important manoeuvres are commanded. Although the 'short-period' equations are the results of a linearization process, the lateral dynamics on pitch and yaw axes can be coupled by the vehicle roll rate. In fact, when the launch vehicle has a not negligible roll rate, an action on the pitch plane produces an effect also in the yaw plane. Neglecting the elastic behaviour of the whole system and the actuation dynamics, the model is just characterized by the following equations (Greensite [1970]):

Lateral forces equations:

$$\dot{v} = -rU_0 + p_0 w - \frac{1}{2}\frac{\rho V_{rel}^2 S_R}{m} \int \frac{\partial C_N(\eta)}{\partial \beta} \beta(\eta) d\eta + g\cos\theta_0 \cdot \Delta\theta + \frac{T_c}{m}\Delta\sigma$$

$$\dot{w} = -p_0 v + U_0 w - \frac{1}{2}\frac{\rho V_{rel}^2 S_R}{m} \int \frac{\partial C_N(\eta)}{\partial \alpha} \alpha(\eta) d\eta - g\sin\theta_0 \cdot \Delta\theta - \frac{T_c}{m}\Delta\varepsilon$$

Moment equations:

$$I_{yy}\dot{q} = -(I_{xx} - I_{zz})\, p_0 r - l_c T_c \Delta\varepsilon + \frac{1}{2}\rho V_{rel}^2 S_R \int \frac{\partial C_N(\eta)}{\partial \alpha}(\eta_{cg} - \eta)\alpha(\eta) d\eta$$

$$I_{zz}\dot{r} = -(I_{yy} - I_{xx}) p_0 q - l_c T_c \Delta\sigma - \frac{1}{2}\rho V_{rel}^2 S_R \int \frac{\partial C_N(\eta)}{\partial \beta}(\eta_{cg} - \eta)\beta(\eta) d\eta$$

The kinematic equations are $\Delta\dot{\theta} = q$ and $\Delta\dot{\psi} = \frac{1}{\cos\theta_0} \cdot r$ where l_c is the distance between the centre of mass and the pivot point; the T_c is the swivelled thrust; $(\rho V_{rel}^2)/2$ is the dynamic pressure; S_R is the reference area. The angle of attack α and the side-slip angle β can be expressed as follows:

$$\alpha(\eta) = \frac{w + w_{wind}}{U_0} - \frac{\eta_{cg} - \eta}{U_0} q$$

$$\beta(\eta) = \frac{v + v_{wind}}{U_0} + \frac{\eta_{cg} - \eta}{U_0} r$$

The states are the lateral launcher velocities (v, w), angular velocities (q, r), yaw and pitch angles (ψ, θ) with $\boldsymbol{X} = (\, v \;\; r \;\; \psi \;\; w \;\; q \;\; \theta \,)^T$ and the inputs are the two nozzles deflections $\boldsymbol{U} = (\Delta\sigma,\, \Delta\varepsilon)^T$.

Using the above equations of motion, different linear time-invariant (LTI) models can be derived for different instants of a flight trajectory by assuming the frozen parameters including the vehicle roll rate p in order to investigate the effect of the roll rate on the system dynamics. Therefore, 36 different models were generated for 9 different flight instants (from $5s$ called Model 1 to $85s$ called Model 9 with an increment of 10 seconds), each of them for 4 roll rates $p_0 = (0, 10, 20, 30)^\circ/s$. Figure 1 shows how the open-loop poles evolve with the roll rate p_0 on model 6. It illustrates that the open loop launcher is naturally unstable. For $p_0 = 0^o/s$ (Δ), the pair of the real positive pole at $+1.7$ and the real negative pole at -1.85 determine the unstable pitch motion. You can also identify a pole at the origin representing the integration of the pitch rate q to the pitch angle θ and one slightly unstable pole at $+0.01$ associated to the lateral drift w. You find more or less the same poles (Δ) for the unstable yaw motion, the yaw angle ψ and the lateral drift v. Both axis are naturally decoupled. With non-zero p_0 however, *i.e.* $+$, the real poles for pitch and yaw motion combine eachother to coupled complex conjugated pole pairs.

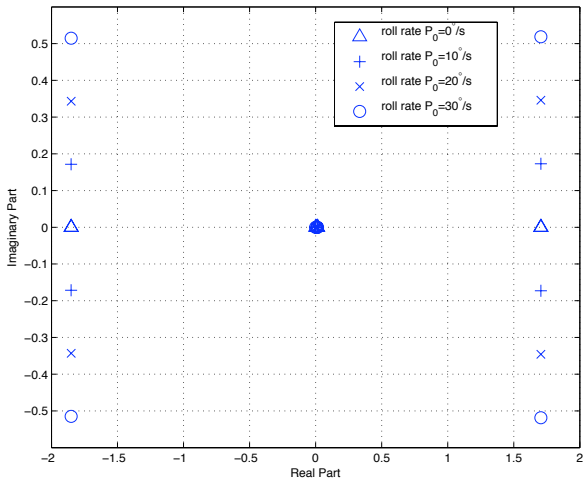

Figure 1. System open-loop poles vs roll rate p_0 (Model 6)

3.2 Specifications

The controlled outputs are the pitch angle θ and the yaw angle ψ. A performance objective for the control law is to follow a unit step in θ (resp. in ψ) with a 90% settling time T_s inferior to 1.8s, an overshoot less than 10% and no steady-state errors.

The decoupling objective is as follows: a command on θ should not affect ψ and reciprocally. So the controller will have to limit the coupling effects.

At last, the controller must be robust to any roll rate variations between $0°/s$ and $30°/s$ and be effective all along the takeoff phase between time 5s and time 85s. In order to be robust to non modelised high-frequency dynamics or flexible effects, the gain margins should remain between 0 dB and 3 dB, and the delay margins greater than 40ms.

3.3 Controller architecture

The available measurements are v, r, ψ, w, q, θ. We add two integral terms on ψ and θ in order to ensure zero steady-state errors on these variables and perturbation robustness. With 8 measurements, we are able to assign 8 poles, see Eq. (2). With two inputs $\Delta\sigma$ and $\Delta\varepsilon$, there are 16 gains K_{ij} as degrees of freedom:

$$\boldsymbol{K} = \begin{bmatrix} K_{11} & K_{12} & K_{13} & K_{14} & K_{15} & K_{16} & K_{17} & K_{18} \\ K_{21} & K_{22} & K_{23} & K_{24} & K_{25} & K_{26} & K_{27} & K_{28} \end{bmatrix} \quad (7)$$

allowing furthermore the axe decoupling following Eq. (3).

3.4 Eigenstructure assignment for the nominal model M_0 = Model 6 with $p_0 = 0°/s$

θ and ψ are naturally decoupled. λ_1, $\lambda_{2,3}$ and λ_4 are belonging to θ and λ_5, $\lambda_{6,7}$ and λ_8 to ψ. During the design **Step A.1**, the low frequency poles λ_1 and λ_5 are chosen near low-frequency zeros in order to compensate non desirable zero effects. $\lambda_{2,3}$ and $\lambda_{6,7}$ satisfy the settling time criterion of 1.8 s. Their damping is 0.7 for an overshoot less than 10%. The fast eigenvalues λ_4 and λ_8 are chosen faster than the complex poles, but not too fast in order to keep gains K_{ij} small. See M_0 in Tab. 1 for more details. The eigenstructure assignment boils down to a pole placement following Eq. (2). This single model controller leads for sure to good time behaviour in terms of settling time and overshoot for the nominal model, but time response analysis during **Step B.1** identifies immediately that it does not ensure decoupling on the other models (it was not taken into account during synthesis) and that oscillations appear for higher roll rates $p_0 \geq 20^o/s$. Model 6 with $p_0 = 20°/s$ is identified as the first worst-case model M_1.

Table 1. Eigenstructure assignments for the three synthesis models

Model		Poles	
Name	Number	Open loop	Closed loop
M_0	#6 $p_0 = 0°/s$	1.71 1.70 0.0158 0.0104 0 0 −1.85 −1.85	$\lambda_1 = -0.046$ $\lambda_{2,3} = -1.4 \pm 1.4i$ $\lambda_4 = -6$ $\lambda_5 = -0.046$ $\lambda_{6,7} = -1.4 \pm 1.4i$ $\lambda_8 = -6$
M_1	#6 $p_0 = 20°/s$	$1.71 \pm 0.346i$ 0.0152 0.01 0 0 $-1.85 \pm 0.343i$	$\lambda_{1,2} = -0.0459 \pm 0.3490i$ $\lambda_{3,4} = -1.4 \pm 1.4i$ $\lambda_5 = -6$ $\lambda_{6,7} = -1.4 \pm 1.4i$ $\lambda_8 = -6$
M_2	#9 $p_0 = 20°/s$	$1.57 \pm 0.521i$ 0.0204 0.0241 0 0 $-1.75 \pm 0.513i$	$\lambda_{1,2} = -0.01 \pm 0.3490i$ $\lambda_{3,4} = -1.4 \pm 1.4i$ $\lambda_5 = -6$ $\lambda_{6,7} = -1.4 \pm 1.4i$ $\lambda_8 = -6$

3.5 Search for a suitable eigenstructure for Model M_1 = Model 6 with $p_0 = 20°/s$

The choice of closed loop eigenvalues and eigenvectors is not as straightforward as the coupling depends on the roll rate p. In order to find a suitable eigenstructure on M_1, it is first decided to treat M_1 independently from M_0, *i.e.* return to **Step A.1** instead of continuing with **Step B.2**. A similar pole placement as for model M_0 with coherent supplementary constraints (3) to decouple θ and ψ does not give expected results. A trial and error approach did not lead to the selection of adequate eigenvalues and eigenvectors.

In order to solve the issue, a LQR design (Kalman [1960]) is then considered with $R = diag(0.001, 0.001)$ and $Q = diag(0, 0.1, 0.1, 1, 0, 0.1, 0.1, 1)$ where $\int\theta$ and $\int\psi$ are the more ponderated states. The LQR controller performed quite well placing the closed loop poles as follows :

$$\begin{aligned} \lambda_{1,2} &= -0.0459 \pm 0.3490i \\ \lambda_{3,4} &= -1.3527 \pm 1.1534i \\ \lambda_{5,6} &= -1.5915 \pm 1.2870i \\ \lambda_{7,8} &= -64.7749 \pm 0.34i \end{aligned} \quad (8)$$

The complex pair of eigenvalues $\lambda_{1,2}$ seems to be critical in the decoupling effect and is located near a multivariable zero. As multivariable zeros are not as well understood as SISO zeros, our former study did not point that out. This complex value must be preserved and calculated by an LQR design for each considered model. It can not be decoupled as for M_0 and is hence affected either to θ or to ψ, here to θ. Finally, an eigenstructure affecting $\lambda_{1,2}$, $\lambda_{3,4}$, λ_5 to θ and $\lambda_{6,7}$, λ_8 to ψ is assigned. The values for $\lambda_i \neq \lambda_{1,2}$ are the same as those for M_0 in order to satisfy settling time and overshoot criteria while keeping gains K_{ij} as small as possible. See M_1 in Tab. 1. Figure 2 shows that all requirements concerning settling time, overshoot and decoupling are satisfied for M_1.

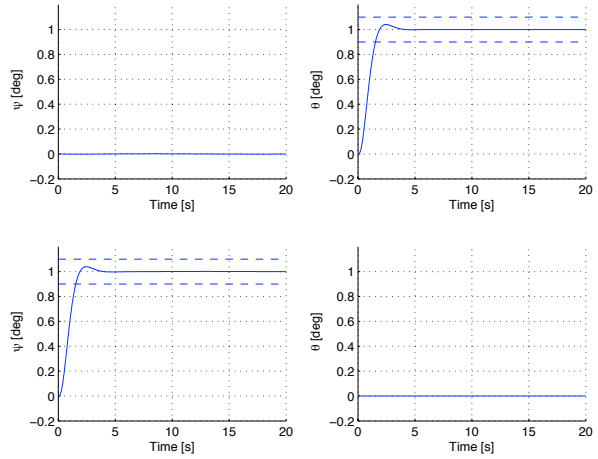

Figure 2. Time responses due to a unit step command in θ_c (up) and in ψ_c (down) with the single model static controller for Model 6, $p_0 = 20°/s$)

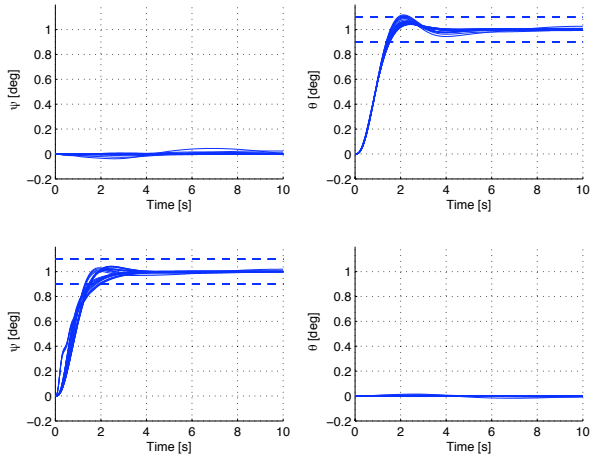

Figure 3. Time responses due to a unit step command in θ_c (up) and in ψ_c (down) with the scheduled controller w.r.t. p (Models 1 to 6)

3.6 Self scheduled controller w.r.t. p

Having identified the suitable eigenstructure assignments for models with zero and non-zero roll rate p_0, it is possible to continue the (Mu-μ)-iterations stopped at the end of §3.4, *i.e.* with **Step B.2**. M_0 and M_1 can be treated simultaneously, if p is introduced as a scheduling parameter. The total roll rate p is normalized as $p = 15 + 15\delta p$ and $\delta p \in [-1, 1]$. The controller is then scheduled as follows :

$$\boldsymbol{K} = \boldsymbol{K_0} + \boldsymbol{K_1}\delta p \tag{9}$$

The self-scheduled controller is synthetized by assigning the eigenvalues of the augmented system:

$$\left(A_\Delta, B_\Delta, \begin{bmatrix} C_\Delta \\ \delta p C_\Delta \end{bmatrix}, \begin{bmatrix} D_\Delta \\ \delta p D_\Delta \end{bmatrix}\right) \tag{10}$$

with $\boldsymbol{K} = [\boldsymbol{K_0}\ \boldsymbol{K_1}]$. $\boldsymbol{K}$ has now $2 \times 16 = 32$ degrees of freedom which can be used to assign two models following Eq. (2). The two former eigenstructure for M_0 and M_1 of Tab.1 are assigned simultaneously on the augmented system. When dealing with M_0, the augmented system (10) is taken with $\delta_p = -1$ whereas $\delta_p = 1/3$ for M_1.

A quick study of the time responses (**Step B.1**) reveals that this scheduled controller performs very well for models 1 to 6 at any roll rates in $[0°/s, 30°/s]$ (Fig.3). Nevertheless the behaviour tends to be quite oscillatory and not satisfactory for models 7 to 9 with rates above $10°/s$(Fig. 4). Depending on the time, the performances of this scheduled controller are hence not acceptable. Model 9 at $p_0 = 20^o/s$ is identified as a second worst case model M_2.

3.7 Self scheduled controller w.r.t. p and t

In order to be able to treat simultaneously models M_0, M_1 and M_2, 16 new degrees of freedom have to be added to Eq. (2) in **Step B.2**. The idea is now to add the time as a supplementary scheduling parameter. The so-scheduled controller has the form:

$$\boldsymbol{K} = \boldsymbol{K_0} + \boldsymbol{K_1}\delta p + \boldsymbol{K_2}\delta t \tag{11}$$

The total time is normalized as $t = 55 + 30\delta t$ and $\delta t \in [0, 1]$ (for model 6, $\delta t = 0$ and for model 9, $\delta t = 1$). The self-scheduled controller is synthetized by assigning the eigenvalues of the augmented system:

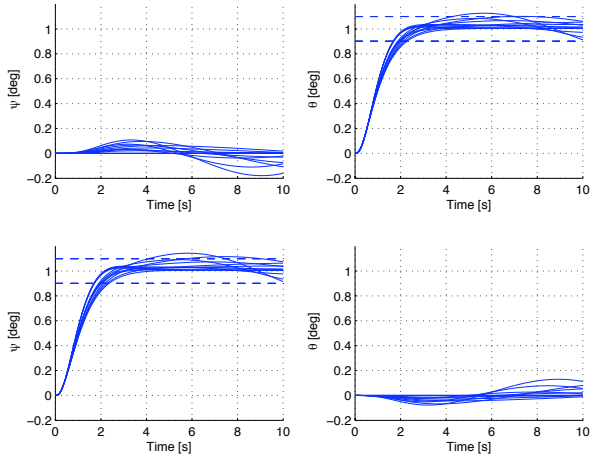

Figure 4. Time responses due to a unit step command in θ_c (up) and in ψ_c (down) with the scheduled controller w.r.t. p (Models 7 to 9)

$$\left(A_\Delta, B_\Delta, \begin{bmatrix} C_\Delta \\ \delta p C_\Delta \\ \delta t C_\Delta \end{bmatrix}, \begin{bmatrix} D_\Delta \\ \delta p D_\Delta \\ \delta t D_\Delta \end{bmatrix}\right) \tag{12}$$

In addition to the former eigenstructure assignments for M_0 and M_1, the assignement for Model 9 with $p_0 = 20°/s$ has to be chosen. The low-frequency poles $\lambda_{1,2}$ are again determined by an LQR approach as for M_1 for the same reasons. The other eigenvalues are chosen as for M_0 in order to respect settling time and overshoot criteria while keeping gains K_{ij} small. Again $\lambda_{1,2}$, $\lambda_{3,4}$ and λ_5 are affected to θ, the remaining 3 to ψ. See M_2 in Tab. 1. Figure 5 shows the result of the time-responses analysis in **Step B.1**. They are now quite satisfactory for all models and roll rates. It is possible to stop the (Mu-μ)-iterations at this point.

Nevertheless, there are still light oscillations and the decoupling could still be improved. One way to improve this behaviour could be to continue the (Mu-μ)-iterations by also treating Model 1 at $t = 5\,s$ as a third worst-case model M_3 during synthesis. This would mean to add an additional term $\boldsymbol{K_3}$ to the controller of Eq. (11) with

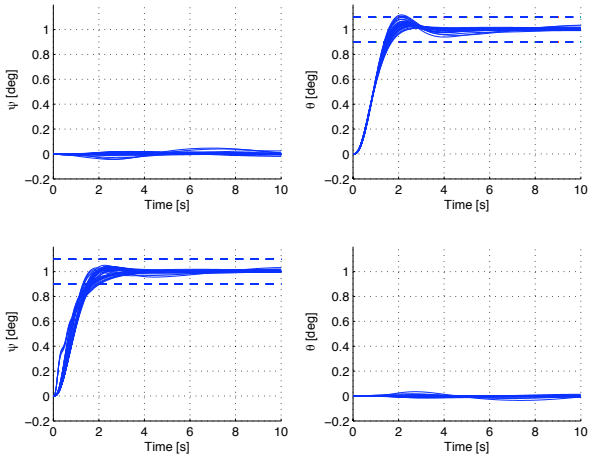

Figure 5. Time responses due to a unit step command in θ_c (up) and in ψ_c (down) with the final scheduled controller

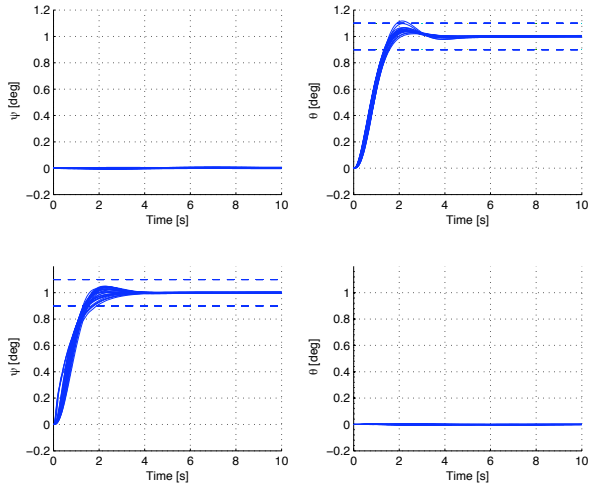

Figure 6. Time responses due to a unit step command in θ_c (up) and in ψ_c (down) with the final improved scheduled controller

an additional parameter δ_3 (for example δt^2) in order to create the necessary degrees of freedom for the control design. Here, a simplier way was chosen.

3.8 Improved self scheduled controller w.r.t. p and t

By speeding up the fast poles of Models 6 and 9, $p_0 = 20°/s$ (instead of $\lambda_{5,8} = -6$, we take $\lambda_{5,8} = -20$ on Model 6 and $\lambda_{5,8} = -30$ on Model 9), one can obtain much better time-responses (Fig 6). But an overshoot can be observed on θ time-responses of Models 1 and 2. As these models were not considered in the eigenstructure assignment, they are not entirely satisfactory but still remain acceptable. Nevertheless, gains are higher compared to the former scheduled controller, see Tab. 2 for the values of K_0, K_1 and K_2. Moreover in presence of a flexible model, such big gains may not give as good results. This will be treated in future work on a flexible model of the launcher. Frequency constraints can be added in the synthesis in order to limit the action of the controller on specific frequencies and/or additional terms can be added to Eq. (11) in order to increase the degrees of freedom.

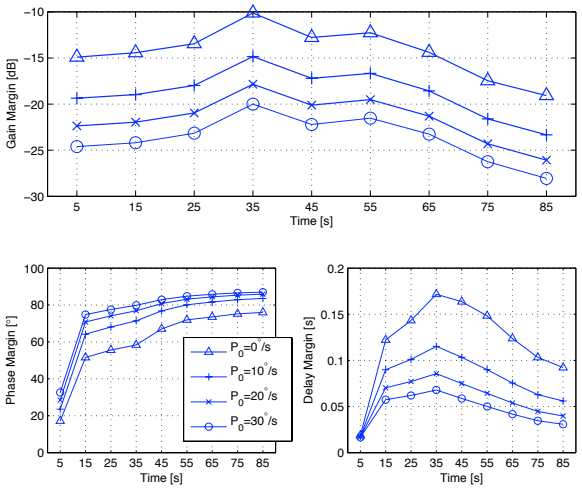

Figure 7. Pitch control loop SISO margins

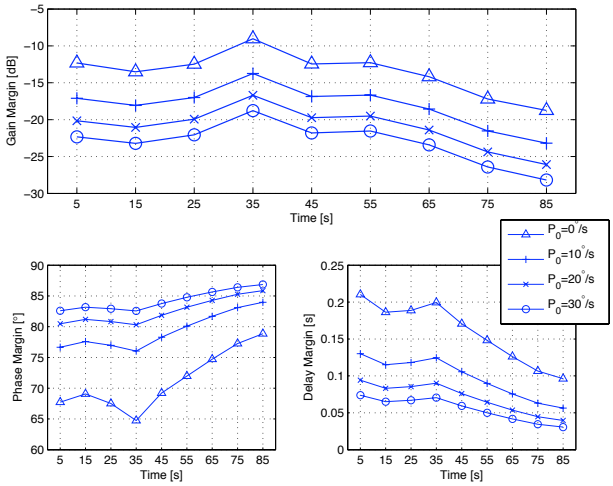

Figure 8. Yaw control loop SISO margins

4. PRELIMINARY ROBUST ANALYSIS

We propose a brief study of the robustness of our improved controller. First SISO margins are calcutated, then MIMO margins.

4.1 SISO margins

Gain, phase and delay margins are found with the improved controller. For the pitch control loop, Figure 7 shows that the gain margins are good compared to the required 3dB margin. The delay margins are rather poor at $p_0 = 30^o/s$, but the specification of $40\,ms$ is satisfied for all models except of Model 1 whose delay margin violates with $25\,ms$ the requirement. Considering the yaw control loop (Fig. 8), all margins are good for any case.

With increasing roll rate p_0, gain and phase margins are improving which seems surprising, but for greater roll rates ($50°/s$ and above), they are decreasing. Nevertheless, SISO margins are quite optimistic and MIMO margins must be calculated.

4.2 MIMO margins

In the SISO approach, there is only one control loop that is disturbed at the same time. Hence the margins found before may not reflect the robustness of the system. The

Table 2. Improved scheduled controller matrices

$$\boldsymbol{K_0} = \begin{bmatrix} 0.0008448 & 2.9753 & 5.8158 & -7.5389 & 0.000003257 & -0.03935 & -0.002092 & 0.001478 \\ 0 & 0.03938 & 0 & 0 & 0.0008568 & 2.9754 & 7.7014 & -9.9936 \end{bmatrix}$$

$$\boldsymbol{K_1} = \begin{bmatrix} -0.0001868 & 1.6203 & 3.5132 & -4.7908 & 0.000003257 & -0.03935 & -0.002092 & 0.001478 \\ 0 & 0.03938 & 0 & 0 & -0.00019802 & 1.6202 & 4.6636 & -6.3509 \end{bmatrix}$$

$$\boldsymbol{K_2} = \begin{bmatrix} -0.0006866 & -0.02936 & 1.4631 & -2.2361 & -0.000003811 & 0.02095 & 0.002041 & -0.001089 \\ 0 & -0.02098 & 0 & 0 & -0.0006931 & -0.02941 & 0.1457 & -0.5455 \end{bmatrix}$$

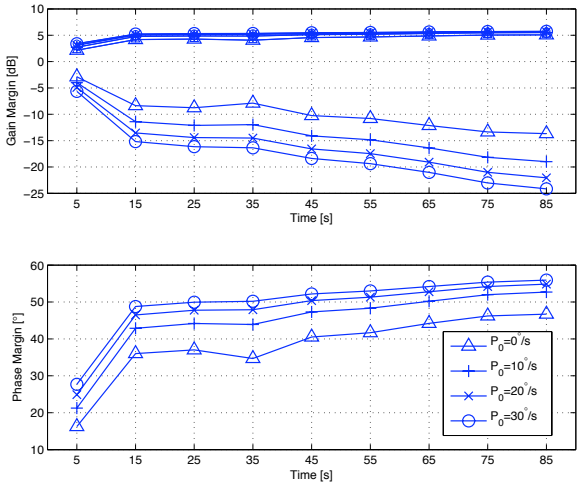

Figure 9. MIMO margins

stability is now studied when perturbations are applied at the input of the system. The perturbations are of the form $I+L_{mde} = diag(k_i e^{j\varphi_i})$. The objective is to calculate the independant margins of gain k_i and phase φ_i by the following formulae:

$$\forall i, \quad |k_i - 1| \leq \alpha \quad \text{and} \quad 2|\sin\left(\frac{\varphi_i}{2}\right)| \leq \alpha,$$

$$\alpha = \sup_{\omega} \left[\bar{\sigma}\left(\left(I + KG\right)^{-1} KG\right)\right]^{-1} \qquad (13)$$

α is first determined, gain and phase margins are then calculated independently. There is a minimum and maximum value for each of them, inside of which the feedback gain loop can vary while letting the system stable. Figure 9 shows that the SISO approach surestimated the gain margins but the margins are still satisfactory. The gain margin is with 5dB still higher than the required 3dB. Concerning the phase margins, they are about 40^o instead of the SISO phase margins with about 60^o. The MIMO phase margin of Model 1 is with 16^o slightly worse than the SISO one with 19^o. Although MIMO margins are inferior to SISO margins, they are still fulfilling the requirements (except for Model 1). As already mentioned, with Model 1 as an additional synthesis model, its margins could be improved.

5. CONCLUSION

In this article a design technique for self-scheduled controllers is applied to a launcher takeoff problem. With a static controller scheduled w.r.t. roll rate p and time t, performance and decoupling objectives are fulfilled for all considered models. Moreover, SISO and MIMO margins satisfy requirements. Considering the number of gains (16) and of models (36), classic gain interpolation could have been more difficult to tackle and the user would have spent more time for computation. In our case, only 3 models needed to be treated at the same time. A LFT model is under study in order to perform a μ-analysis that will confirm our results.

ACKNOWLEDGEMENTS

We thank Piero D. Resta (VEGA LV Avionics Chief Eng., from ESA/IPT) for useful discussions and advices, and Sabrina Labbad for obtaining the main results.

REFERENCES

D. Alazard, N. Imbert, Clément, and P. Apkarian. Launcher attitude control: some additional and optimization tools. In *CNES/EADS Conference on Launcher Technology, Madrid*, November 2003.

G. Constant, S. Chable, C. Chiappa, and C. Döll. Robustification of an h_2 autopilot for flexible aircraft by self scheduling based on multi model eigenstructure assignment. In *International Council of Aeronautical Sciences*, pages 542.1–542.9, 2002.

C. Döll, Y. Le Gorrec, G. Ferreres, and J. F. Magni. A robust self-scheduled missile autopilot: Design by multimodel eigenstructure assignment. *Control Engineering Practice*, 9(10):1067–1078, October 2001.

L. Greensite. *Analysis and design of space vehicle control system.* New York: Spartan Books, 1970.

R. E. Kalman. Contribution to the theory of optimal control. *Bol. Soc. Mat. Mex.*, 5:102–119, 1960.

J. F. Magni. Multimodel eigenstructure assignment in flight-control design. *Aerospace Sciences and Technologies*, 3(3):141–151, 1999.

J. F. Magni. *Robust modal control with a toolbox for use with matlab.* Kluwer Academic/Plenum Pusblisers, 2002.

J. F. Magni and C. Döll. A new lower bound of the mixed structured singular value. In *Proc. 2nd Asian Control Conference, Seoul, South Corea*, volume I, pages 847–850, 1997.

J. F. Magni, Y. Le Gorrec, and C. Chiappa. A multimodel-based approach to robust and self-scheduled control design. In *37th IEEE Conference on Decision and Control, Tampa, Florida*, pages 3009–3014. IEEE, 1998.

A. Packard and J. C. Doyle. The complex structured singular value. *Automatica*, 29(1):71–109, January 1993.

C. Roux and I Cruciani. Roll coupling effects on the stability margins for vega launcher. In *AIAA Guidance, Navigation, and Control Conference and Exhibit, South Carolina*, number 6630, 2007.

M. Sadray and R. Colgreb. Uav flight simulation: credibility of linear decoupled vs. nonlinear coupled equations of motion. In *AIAA Modelling and Simulation Technologies Conference and Exhibit, San Francisco, USA*, 2005.